Ultrathin Triblock Copolymer Films on Tailored Polymer Brushes

Igor Luzinov*,† and Vladimir V. Tsukruk*,‡

School of Materials Science and Engineering, Clemson University, Clemson, South Carolina 29634, and Department of Materials Science & Engineering, Iowa State University, Ames, Iowa 50011

Received April 12, 2002

ABSTRACT: We fabricated ultrathin poly[styrene-*b*-butadiene-*b*-styrene] copolymer (SBS) films deposited on polystyrene brushes. The thickness of the films was kept constant, while the grafting density and molar mass of the grafted polymer layers were varied to reveal the influence of the brush interface on the structure of the films. We examined the surface morphology of the films formed and found a strong effect of the underlying brushes on the formation of the SBS films. The development of a zeroth layer (layer without internal microphase separated structure) of SBS on the top of the grafted layer was observed. Both polystyrene and polybutadiene blocks were present inside the zeroth layer. The first block copolymer layer formed on top of the zeroth layer possessed the surface microstructure typical for the block copolymer in the bulk state. The polymer brushes were actively involved in the formation of the zeroth layer, and the structure of the block copolymer films was influenced by the grafting density and degree of polymerization of the underlying grafted polymer layer. We observed significantly distinct morphologies for the copolymer films of the same thickness deposited on the different polymer brushes. Morphology of isolated islands, holes of different size, and intermediates between islands and holes as well as uniform zeroth layer developed during annealing. Our studies demonstrate that the morphology of ultrathin block copolymer film can be manipulated by the grafting density and molecular mass of the underlying brush.

Introduction

Theoretical and experimental studies have been devoted to thin polymer films made of block copolymers due to their potential applications in many technological areas, including coatings, nanolithography, microelectronics, lubricants, adhesives, and membrane separation.[1] These films self-organize in a variety of ordered microdomain structures from spherical to lamellar as the fraction and molar mass of blocks constituting the copolymers are changed. The microdomain orientation of the films is strongly influenced by the boundary conditions at polymer−substrate and polymer−air (vacuum) interfaces.[1−6] This behavior is connected with a preferential segregation of the blocks to a substrate and a free surface. The ordering of the microdomain morphology depends on the relative surface energy of each block and substrate.[3,5,7−12] Therefore, the structure of the film may be manipulated, if the surface parameters of substrate are under precise control.

Mansky et al.[2,7,9] and Huang et al.[1,8,10,11] used random copolymer brushes chemically end-grafted to the surface to systematically change the interaction between the symmetric diblock copolymer and substrate. Their approach allowed controlling nanostructures within films. Harrison et al.[13] showed that attaching a buffer layer of polystyrene brushes to silicon wafer surface changed the substrate wetting conditions for poly[styrene-*b*-butadiene-*b*-styrene] (SBS) and poly[styrene-*b*-butadiene] (SB) block copolymers.

Recently, Harrison et al.[13,14] introduced a concept of a "zeroth" layer (layer without internal ordered microphase-separated structure) for block copolymer deposited on the substrate as an uniform layer in vicinity of the surface. The layer thickness was suggested to be less than the equilibrium spacing of the microdomain structure for the given copolymer. Zeroth layer formation was experimentally detected by SEM for SBS deposited on PS brush and related to the interaction between the block(s) of the copolymer and the brush surface.[13] It was reported that block copolymer layers with the thickness of 20 nm spin-coated on brush-coated wafers produced the uniform zeroth layer of SBS without formation of islands and holes after annealing. Spin-coating a slightly thicker film produced the typical islands of microphase-separated structure on top of the zeroth layer, indicating the formation of well-organized "first" layer on the top of the primary block copolymer film. Indeed, the zeroth layer was suggested as a directing interface between the polymer brush and relatively thick block copolymer films.

When a block copolymer is brought into contact with the homopolymer brush at an elevated temperature, the polymer brush is wetted by that portion of the block copolymer that comprises the monomer used for the brush synthesis. This results in a reduction in the interfacial tension.[7] At this point, the block copolymer chains may penetrate into the brush. The penetration is prohibited only for the brushes with high grafting density, when a so-called a "dry" brush regime is reached.[15,16] In other cases, the extent of the penetration should be dependent on the grafting density and molar mass of the chains constituting the block and brushes.[16,17] The level of the penetration should affect the thickness and structure of the zeroth layer and, consequently, the self-organization of the block copolymer in thin film.

Generally, modification of the film−substrate interface with polymer brushes gives the ability to create a surface that consists of the monomer as found in a particular copolymer. This provides tuneability over a wide range of surface affinity.[7] A polymer brush at the interface reduces the entropic driving force for dewetting

† Clemson University.
‡ Iowa State University.
* To whom correspondence should be addressed: e-mail luzinov@clemson.edu and vladimir@iastate.edu.

10.1021/ma0205818 CCC: $22.00
Published on Web 06/13/2002

and improves adhesion. Largely, this ultrathin grafted film directs the formation of the very first block copolymer monolayer, which is in a contact with the surface and is a guide for the microdomain orientation.

The present work focused on study of the formation of the zeroth layer of SBS on the top of a grafted polystyrene brush. The grafting density and molar mass of the polymer brush were varied to find out whether these parameters of the brush interface might be instrumental in control of the zeroth layer development. We previously showed that smooth and uniform polystyrene layers of different density and molar mass could be grafted to a silicon surface through epoxysilane monolayers deposited on the substrate.[18] To avoid the formation of multilayered structures, the SBS film with the thickness less than the equilibrium spacing of the microdomain structure for the given copolymer was spin-coated on the substrate covered with the grafted PS. Our objective was to determine whether the grafted polymer layers serve as impenetrable boundary for block copolymers that reduces interfacial tension between the copolymer and the surface or whether the layers act or are involved in the process of zeroth layer formation through the penetration of the copolymer blocks into the brush.

Experimental Section

The epoxysilane compound (3-glycidoxypropyl)trimethoxysilane was purchased from Gelest Inc. ACS grade toluene and ethanol were obtained from Aldrich and were used as received. Highly polished single-crystal silicon wafers of {100} orientation (PureSilicon, Inc.) were used as substrates. Carboxy-terminated polystyrenes of different molar mass were obtained from Polymer Source, Inc. (M_n = 45 900 and 672 000 g/mol) and Aldrich (M_n = 143 000 g/mol). The samples possessed a relatively narrow molar mass distribution with M_w/M_n in the range 1.05−1.4. Phthalic anhydride-terminated PS was synthesized at the Institute of Polymer Research Dresden (Germany) (M_n = 11 900 g/mol, M_w/M_n = 1.42).[18] SBS triblock copolymer was purchased from Aldrich. It has a M_w = 140 000 g/mol, M_w/M_n = 1.2, and PS weight fraction = 30%.[19] Although the polydispersity of 1.2 is relatively high, we did not notice irreproducibility in our experimental results.

The silicon wafers were first cleaned in an ultrasonic bath for 30 min, placed in a hot piranha solution (3:1 concentrated sulfuric acid/30% hydrogen peroxide) for 1 h, and then rinsed several times with high-purity water (18 MΩ cm, Nanopure). After rinsing, the substrates were dried under a stream of dry nitrogen, immediately placed into a nitrogen-filled glovebox, and immersed in an epoxysilane solution (1 vol %) for 24 h. After the deposition was complete, the modified substrates were removed from the solution, rinsed several times with toluene and ethanol, and dried overnight. The initial polymer film was spin-coated from 1 wt % toluene solution onto the silicon wafers modified by the epoxysilane SAM. The thickness of these polystyrene films measured by ellipsometry was 40 ± 5 nm. The specimens were placed in a vacuum oven at 150 °C to enable the end groups to graft to the epoxy-terminated substrate. The unbonded polymer was removed by multiple washing with toluene, including washing in an ultrasonic bath. We varied the grafting time to prepare the grafted films with different grafting density. A detailed description of the fabrication of epoxy-terminated SAMs and grafted PS layers can be found in our previous publications.[18,20] SBS film was spin-coated from the toluene solution onto the wafer modified by the grafted PS layers. The thickness of the spin-coated film measured by ellipsometry was 32 ± 3 nm. The films were thinner than the equilibrium spacing of the microdomain structure for the given copolymer.[21] The specimen was placed in a vacuum oven at 130 °C for 60 min for annealing. Sample preparation was conducted under clean-room 100 conditions.

Polystyrene layers were examined by a static contact angle (sessile droplet) using a custom-designed optical microscopic system. Ellipsometry was performed with a COMPEL automatic ellipsometer (InOmTech, Inc.) at an angle of incidence of 70°. Original silicon wafers from the same batch and silicon wafers with SAM layer were tested independently and used as reference samples for the analysis of grafted polymer layers and SBS films. Scanning probe microscopy (SPM) studies were performed on a Dimension 3000 (Digital Instruments, Inc.) microscope according to a procedure described earlier.[22,23] We used the tapping and phase modes to study the surface morphology of the films in ambient air. Silicon tips with spring constants of 50 N/m were used. Imaging was done at scan rates in the range 1−2 Hz. The free amplitude for scanning probe, A_0, was chosen about 40 nm. For "light" and "hard" tapping modes, the set-point amplitude ratio, $r_{sp} = A_{sp}/A_0$ (A_{sp} is the set-point amplitude used for the feedback control), was selected to be 0.9 ± 0.05 (amplitude damping of 4 nm) and 0.45 ± 0.05 (amplitude damping 22 nm), respectively.[24−26] The amplitude and phase variation showed that, at $r_{sp} > 0.85$, we scanned at attractive interaction regime. The repulsive mode was in place at $r_{sp} = 0.45$. The root-mean-square (rms) roughness of samples was evaluated from SPM images recorded in light tapping mode. The rms roughness is the standard deviation of feature height (Z) values within a given area:[27]

$$\text{roughness} = \sqrt{\frac{\sum_{i=1}^{N}(Z_i - Z_{ave})^2}{N}} \quad (1)$$

where Z_{ave} is the average Z value within the given area, Z_i is the current Z value, and N is the number of points within a given area.

To characterize the polymer layer, several parameters have been evaluated.[28] The surface coverage, Γ (mg/m^2), was calculated from the ellipsometry thickness of the layer h (nm) by the following equation:

$$\Gamma = h\rho \quad (2)$$

where ρ is density of polystyrene (1.05 g/cm^3).[29]

The grafting density, Σ (chain/nm^2), i.e., the inverse of the average area per adsorbed chain, was determined by

$$\Sigma = \Gamma N_A \times 10^{-21}/M_n = (6.023\Gamma \times 100)/M_n \quad (3)$$

where N_A is the Avogadro's number and M_n (g/mol) is the number-average molar mass of the grafted polymer.

The distance between grafting sites, D (nm), and dimensionless grafting density, σ, were calculated using the following equations:

$$D = (4/\pi\Sigma)^{1/2} \quad (4)$$

$$\sigma = (a/D)^2 \quad (5)$$

where a is the statistical segment length ($a \approx 0.6$ nm for PS[30]).

The radius of gyration for the PS−COOH macromolecules was estimated by the equation[31]

$$R_g = a(N/6)^{1/2} \quad (6)$$

where N is the degree of polymerization.

Results

Grafted Polymer Layers. First, we prepared a variety of polymer brushes with different grafting parameters. The brushes had different molar masses ranging from 11 940 to 672 000 g/mol. We changed the grafting density for each polymer grafted to reveal the effect of this factor on the formation of the zeroth SBS

Table 1. Characteristics of PS Grafted Polymer Layers

sample	N	M_n, g/mol	$2R_g$, nm	thickness, nm
PS-1(1)	115	11 940	5.2	2.3
PS-1(2)	115	11 940	5.2	4
PS-2(1)	440	45 800	10.6	8
PS-3(1)	1373	143 000	21.5	1
PS-3(2)	1373	143 000	21.5	2.7
PS-4(1)	6452	672 000	37.0	1.2
PS-4(2)	6452	672 000	37.0	4

Table 2. Parameters of PS Grafted Polymer Layers

sample	$N^{-1/2}$	$N^{-4/3}$	Σ, chains/nm^2	σ	D, nm	Γ, mg/m^2
PS-1(1)	0.093	0.0018	0.12	0.034	3.2	2.4
PS-1(2)	0.093	0.0018	0.21	0.060	2.5	4.2
PS-2(1)	0.048	0.0003	0.11	0.031	3.4	8.4
PS-3(1)	0.027	7×10^{-5}	0.004	0.0013	17	1.1
PS-3(2)	0.027	7×10^{-5}	0.012	0.0034	10.3	2.8
PS-4(1)	0.0125	8×10^{-6}	0.001	0.0003	33.6	1.3
PS-4(2)	0.0125	8×10^{-6}	0.004	0.0011	18.4	4.2

layer. The characteristics of these grafted polystyrene layers are given in Table 1. The thickness of the grafted film varied from 1 to 8 nm, and the grafting density was changed by more than 1000 times from 0.001 to 0.2 chains/nm^2 (Table 2).

Zhulina et al.[32] developed a scaling theory arguments leading to construction of a diagram of states for macromolecular chains end-grafted to a surface. Three major structural regimes were identified: isolated polymer chains, pinned micelles (well-defined, stable clusters), and homogeneous grafted layer. The formation of the structures was dependent on degree of polymerization, grafting density, and solvent quality. For the case of bad solvent where the solvent is completely expelled from the polymer, the pinned micelles are stable when[33]

$$N^{-4/3} = \Sigma_I < \Sigma < \Sigma_{II} = N^{-1/2} \quad (7)$$

At $\Sigma \ll \Sigma_I$, the chains form individual single chain globules whereas at $\Sigma \gg \Sigma_{II}$ the pinned micelles coalesce into a homogeneous, collapsed grafted layer. SPM allows distinguishing between the structural regimes.[30,33,34] Koutos et al.[33] presented SPM images of end-grafted polystyrene monolayers and demonstrated that at low and moderate grafting densities the experimental results agreed with the scaling arguments and can be situated correctly to the corresponding diagram of states for the single chains and pinned micelles, respectively. However, it was noted that increasing in grafting

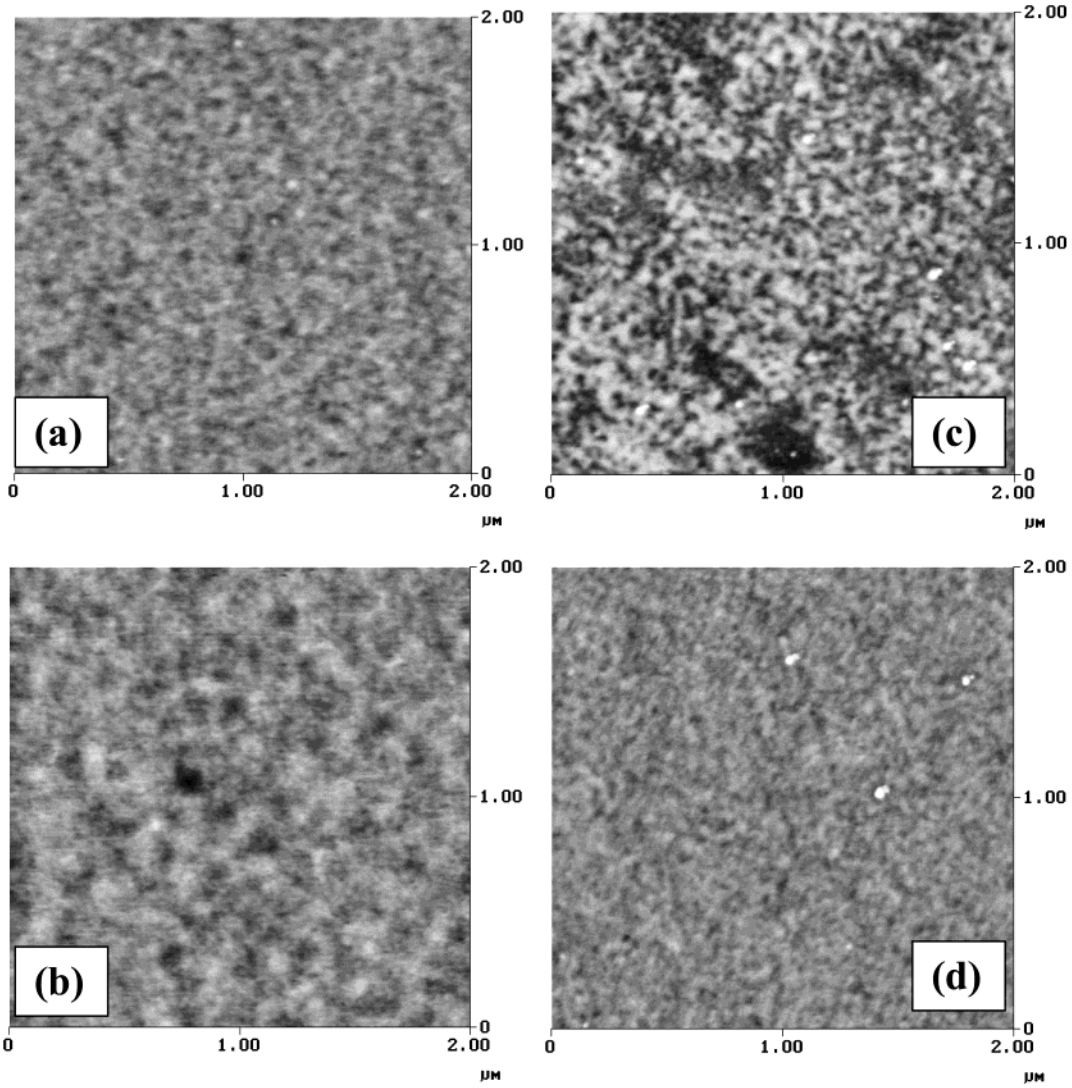

Figure 1. SPM topographical images of PS grafted polymer layers for different molar masses and grafting densities: PS-1(1) (a), PS-2(1) (b), PS-4(1) (c), and PS-4(2) (d). Bright parts correspond to higher features. The vertical scale is 10 nm. The roughness of the layers was comparable for all samples and ranged from 0.25 to 0.38 nm within a 2×2 μm^2 area.

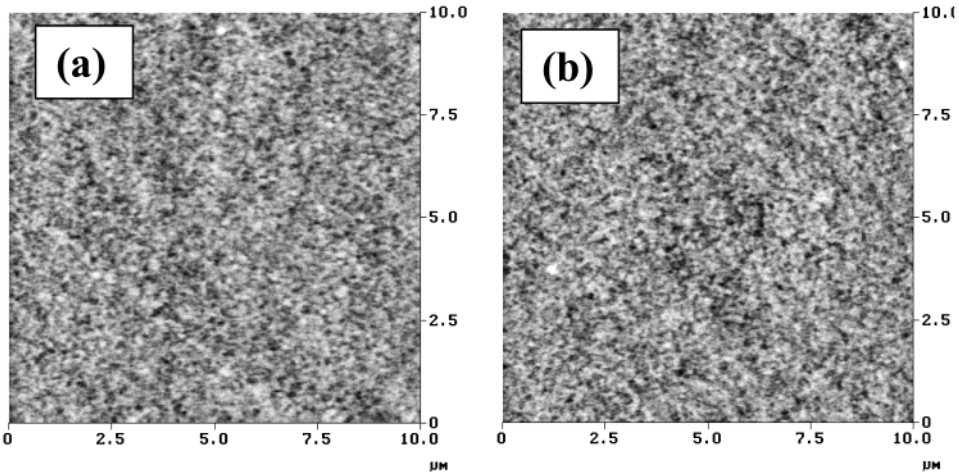

Figure 2. SPM topographical images of SBS films spin-coated over PS grafted polymer layers: PS-1(2) (a) and PS-4(1) (b). Bright parts correspond to higher features. The vertical scale is 10 nm. Scanning at high set point. The microroughness of the films measured by SPM within 2 μm $\times$ 2 μm is 0.30 $\pm$ 0.03 nm, which is much lower than their thickness of 35 nm.

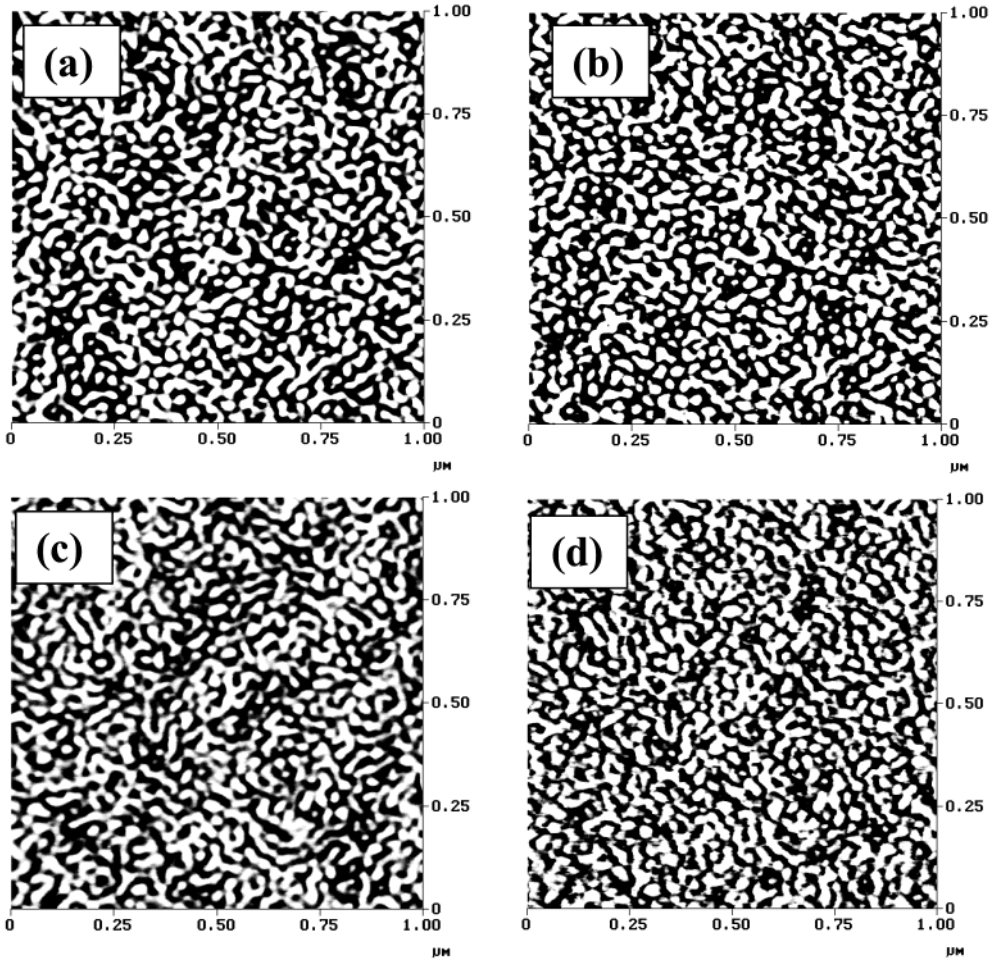

Figure 3. High-magnification SPM topographical (a and c) and phase images (b and d) of SBS films spin-coated over PS grafted polymer layer: PS-1(2) (a, b) and bare silicon wafer (c, d). The vertical scale is 5.0 nm and 20° for topography and phase modes, respectively. Bright parts correspond to higher features and phase shift. Scanning at low set point. Both topography and phase images indicate similar microphase separation within the films deposited over the different PS layers and bare silicon.

density resulted in a structural regime of semicontinuous dimples covering the surface. It is necessary to stress that the dimple regime was observed for $\Sigma < N^{-1/2}$ ($\Sigma/N^{-1/2} \approx 0.5$). The authors pointed that the dimpled morphology corresponded to the regime intermediate between the pinned micelle and the homogeneous layer regime, which simple scaling analysis failed to capture.

Figure 1 presents typical topographical images of the polymer layers for different molar masses and grafting densities. Since the polymers were in a poor solvent (air) and tethered to the surface, the chains collapsed but did not dewet the epoxy-modified surface. The grafting density for all polymer layers synthesized in the present work was well above $N^{-4/3}$ (Table 2). Indeed, according

to the scaling predictions, the single chain regime morphology was not observed in the experiment. Beside PS-3(1) and PS-4(1) samples, the grafting densities of our layers were fairly close to ($\Sigma/N^{-1/2} \approx 0.3-0.5$) or higher than $N^{-1/2}$ (Table 2). These collapsed brushes formed densely packed nanometer-scale clusters distributed homogeneously (Figure 1a,b,d). The layers effectively demonstrated the dimpled morphology of cooperatively collapsed pinned micelles close to observed for the brush with comparable grafting density in ref 33. However, in our case the polymer clusters (pinned micelles) completely covered the substrate. It indicated that the micelles were sufficiently deformed and spread on the substrate surface. The polymer−surface interaction was energetically more favorable than the polymer−air interaction; thus, the clusters wetted and adsorbed on the epoxy-modified surface.[35] For relatively low grafting densities (PS-3(1) and PS-4(1)), the larger clusters were irregularly distributed on the surface (Figure 1c).

The roughness of the films was comparable for all samples and ranged from 0.25 to 0.38 nm within 2 × 2 μm^2 area. The contact angle for all layers was in the range of 86−90°. These numbers are close to the value reported for PS surface (90°).[36] Therefore, both roughness and surface energy of the polymer brushes were quite similar and should not critically affect surface morphology of SBS film deposited over the brush.

SBS Films before Annealing. Figure 2 shows the topographical and phase images for the SBS films deposited on the surface of different PS brushes before annealing. The images were recorded using the tapping mode at the highest set point value (the lowest forces) that permitted a reproducible imaging ($r_{sp} = 0.9 \pm 0.05$, "light" tapping). In this case, we scanned at attractive interaction regime, and consequently, the image reflects the morphology of the topmost layer.[24] The microroughness of the films measured by SPM under these conditions within 2 μm × 2 μm is 0.30 ± 0.03 nm, which is much lower than their thickness. This observation revealed that the film uniformly covers the substrate. Figure 3 presents higher magnification topographical and phase images of the SBS films, recorded in repulsive mode ($r_{sp} = 0.45 \pm 0.05$). This type of tapping (high forces) allows observation of microphase separation that forms underneath the topmost soft polybutadiene layer.[11] At these scanning conditions, hard polystyrene domains of the block copolymers appear brighter in the height and phase images.[24,26,37] Both topography and phase images indicate similar microphase separation within the films deposited over the different PS layers. The small and irregularly shaped PS domains can be clearly observed. SPM images (Figure 3c,d) of the SBS film of a comparable thickness spin-coated on bare silicon wafers reveal that the structure of the film deposited on PS brush and bare silicon have practically the same surface and internal morphology. The Fourier transform of the images shows that typical spacing of phase-segregated structure is 27−30 nm for all samples. Thus, all films have practically the same initial organization before the annealing.

SBS Films after Annealing. Figures 4 and 5 show the topographical images for the surfaces of the SBS films after the annealing at 130 °C. For the film deposited on the top of grafted polymer layer with $M_n = 143\,000$ and $\sigma = 0.003$ the formation of only zeroth layer was found (Figure 5b). This layer was smooth and had a uniform thickness after the annealing. For all other samples, morphology of isolated islands, holes of different size, and intermediate between islands and holes (Figure 5d) developed during annealing. Indeed, the polymer brushes were actively involved in the formation of the zeroth layer, and the microstructure of the block copolymer films was influenced by the

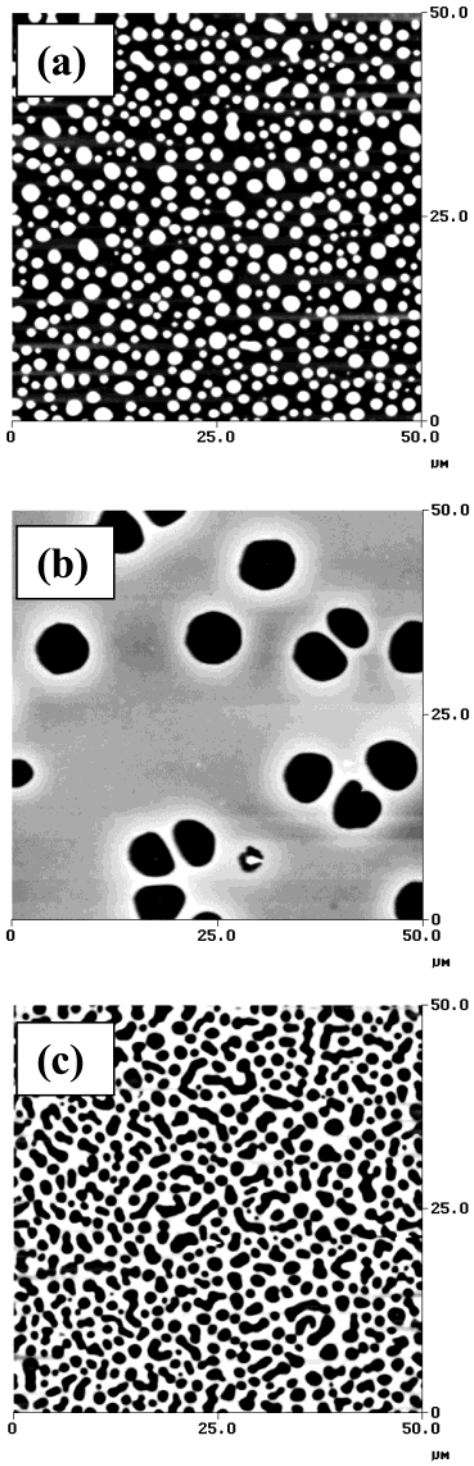

Figure 4. SPM topographical images of the SBS films after annealing. The films were deposited over PS-1(1) (a), PS-1(2) (b), and PS-2(1) (c), which represent a change in grafting density and molar mass of the underlying polymer brush. Morphology of isolated islands (a) and holes of different size (b and c) developed during annealing. Bright parts correspond to higher features. The vertical scale is 70 nm. Scanning at high set point.

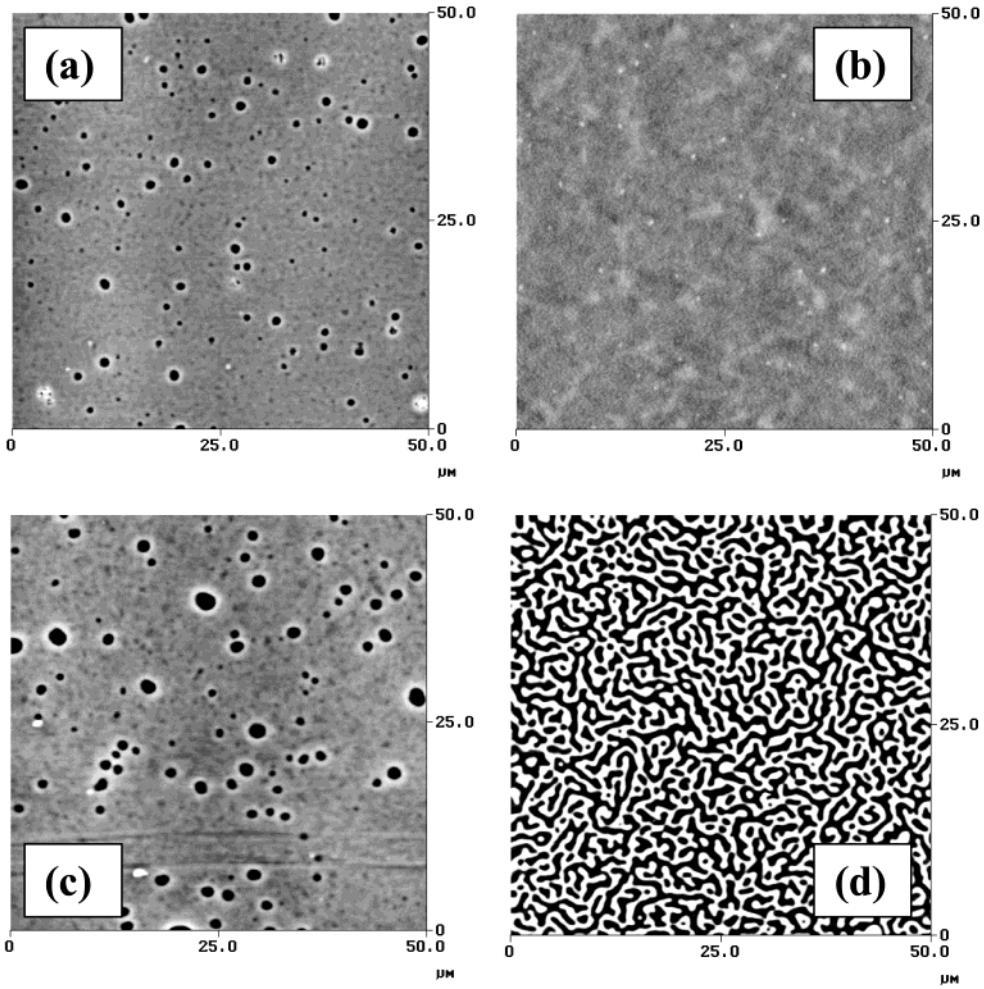

Figure 5. SPM topographical images of the SBS films after annealing. The films were deposited over PS-3(1) (a), PS-3(2) (b), PS-4(1) (c), and PS-4(2) (d), which represent a change in grafting density and molar mass of the underlying polymer brush. Morphology of holes of different size (a and b) and intermediate between islands and holes (d) developed during annealing. For the film deposited on the top of grafted polymer layer with $M_n = 143\,000$ and $\sigma = 0.003$ (b) the formation of only zeroth layer was found. Bright parts correspond to higher features. The vertical scale is 70 nm. Scanning at high set point.

grafting density and degree of polymerization of the underlying grafted polymer layer. Typical height profiles of different morphologies obtained are shown in Figure 6. The height of the islands and depth of the holes are very close within the same sample and represent the thickness of the first well-organized layer being formed.

Figure 7 shows a higher magnification topographical and phase image of SBS film produced on the top of the brush ($M_n = 143\,000$ and $\sigma = 0.001$). The images were recorded in the repulsive mode. One can see the formation of characteristic microphase-separated structures on the zeroth layer. It should be noted that the phase image presented in Figure 7c had a contrast, where PS blocks appear dark. This was different from what was typically observed in this work for the "hard tapping" (scanning in the repulsive mode) of SBS material (see Figure 3). However, the height contrast remained the same for all images taken. It is necessary to notice that this particular image was recorded with very low set point ratio ($r_{sp} = 0.35$). For other images reported here the set point ratio of 0.45 was used. Magonov et al.[38] reported for the poly(diethylsiloxane)/silicon system that as the interaction of the tip and sample increased (set point become smaller), the height contrast remained relatively constant, while phase images could undergo several contrast variations. Bar et al.[25] also described the height and phase contrast variation when the set point was lowered. Pickering and Vansco[26] observed this phenomenon for the polystyrene-*b*-polyisoprene-*b*-polystyrene block copolymer, which have properties close to SBS used in the present work. The PS blocks of the copolymer appeared bright at higher set point but turned dark on phase image if r_{sp} approached 0.4. But, the height contrast remained unchanged at these ($r_{sp} \approx 0.4$) scanning conditions. It was pointed that when the set point was lowered, the cantilever passed from attractive into repulsive regime. Material properties such as stiffness and viscoelastisity resulted in modulation of the amplitude. Since PS has a higher modulus than rubbery phase of block copolymer, the amplitude would be effectively lower in PS regions. This resulted in a contrast where the stiffer regions have an effectively higher topology. This effect was not altered with further set point decrease. Conversely, the phase image contrast, dependent on the tip−sample contact area and contact time, underwent contrast variation as the set point was lowered. It appeared that for the rubber/stiff block copolymer system the tip−sample interaction become higher for rubbery blocks than for stiff domains, when a very low set point was reached.

Figure 8 presents the higher magnification SPM images for the SBS film deposited on the top of grafted polymer layer with $M_n = 143\,000$ and $\sigma = 0.033$, when the formation of only zeroth layer is found. Figure 8a,b

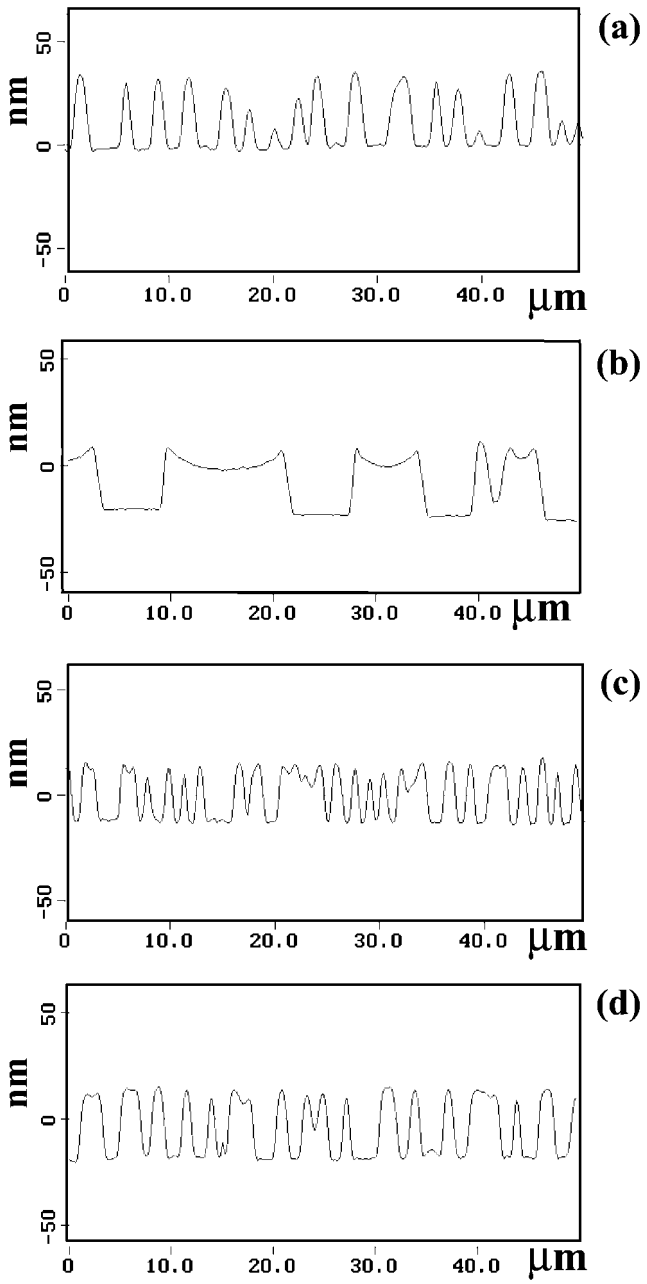

Figure 6. Height profile for the SBS films after annealing. The films were deposited over PS-1(1), PS-2(2), PS-4(2), and PS-2(1). The height of the islands and depth of the holes are very close within the same sample and represent the thickness of the first layer being formed.

shows the topographical and phase images for the layer recorded using the tapping mode at the highest set point value (the lowest forces) that permitted a reproducible imaging ($r_{sp} = 0.9 \pm 0.05$, "light" tapping). In this case, we scanned at the attractive interaction regime, and consequently, the image reflects the morphology of the layer surface.[24] The images demonstrate that the copolymer forms irregularly shaped domains distributed without any order and completely covering the surface (Figure 8a,b). There are no signs of the formation of cylindrical or lamella structures typical for the block copolymer material. It can be speculated that surface of the zeroth layer is covered with only PB block of SBS. We made this conclusion based on literature data,[13,25,39] showing that blocks with lower surface energy (PB in our case) cover the topmost surface.

The images presented in Figure 8c,d were recorded at higher forces that allowed observation of structure formed underneath the topmost soft PB layer.[24] The tip can squeeze the rubbery PB part of the film, and the harder polystyrene part of the block copolymers should appear brighter in the height image. It can be seen from Figure 8c that both PS and PB chains are present inside the zeroth layer. Phase image corroborates this conclusion (Figure 8d). We associated bright areas with "free" PS blocks, which are not involved into the brush. Then, dark areas correspond to PB blocks of the copolymer chains with both PS blocks penetrated inside the brush. Thus, the zeroth layer contains block copolymer chains with one PS block or both PS blocks penetrated inside the brush.

Discussion

As a polymer grafted layer is in contact with a compatible melt, the structure of a polymer brush and the conformation of the grafted chains result from a balance between two effects.[16] Osmotic effects account for monomer−monomer interactions between grafted chains and tend to swell the brush. The elasticity of the grafted chains, on the contrary, tends to diminish the brush extension. When the grafted density is high and chains constituting the brush are elongated, the penetrating polymer melt may be expelled from the brush completely and the dry brush regime is reached. The polymer solvent is expelled when the grafting density σ is high enough depending on the polymerization index of grafted chains, N, and of free chains, P: $\sigma > P^{-1/2}$ ($P < N$) for small free chains and $\sigma > N^{-1/2}$ ($P > N$) for long free chains.[16,40,41] For all grafted polymer films studied here the values of σ is much lower than $N^{-1/2}$ (Table 2) and $P^{-1/2}$. (For P we use the value of the degree of polymerization of PS block of SBS copolymer, which may go inside the polymer brush; $P = 201$ and $P^{-1/2} = 0.071$.) Accordingly, the penetration of the PS block inside the brush is a favorable process, and the formation of zeroth layer should be associated with the incorporation of the block within the layer of the grafted polymer chains.

Nonsymmetric block copolymers form the layered structure from substrate surfaces, similar to the layering observed for the lamellar block copolymers.[13,14,42] Thickness quantization for the spherical or cylindrical domains of the block copolymers comes out from this layered arrangement. Consequently, if the initial thickness does not match a natural period of the microdomain morphology islands and holes will be formed on the surface. For the case when part of the block copolymer is involved in zeroth layer formation, the thickness of the film without holes or island can be approximated from the following expression:[42]

$$t = \alpha n + \beta \tag{8}$$

where t is the thickness of the film, α is the thickness of a domain layer, β is the thickness of zeroth layer, and n is integer. When n equals 1, then the film with the structure shown in Figure 9a is produced. In this case, zeroth and complete first layers are formed on the top of polymer brush. If the thickness of the film is less than α, three different morphologies of the block copolymer film may be found (Figure 9b−d). First of all, uniform zeroth layer, without the development of islands and holes, can be made (Figure 9b). If $\beta < t < \alpha + \beta$, the islands (Figure 9c) or holes (Figure 9d) can be observed.

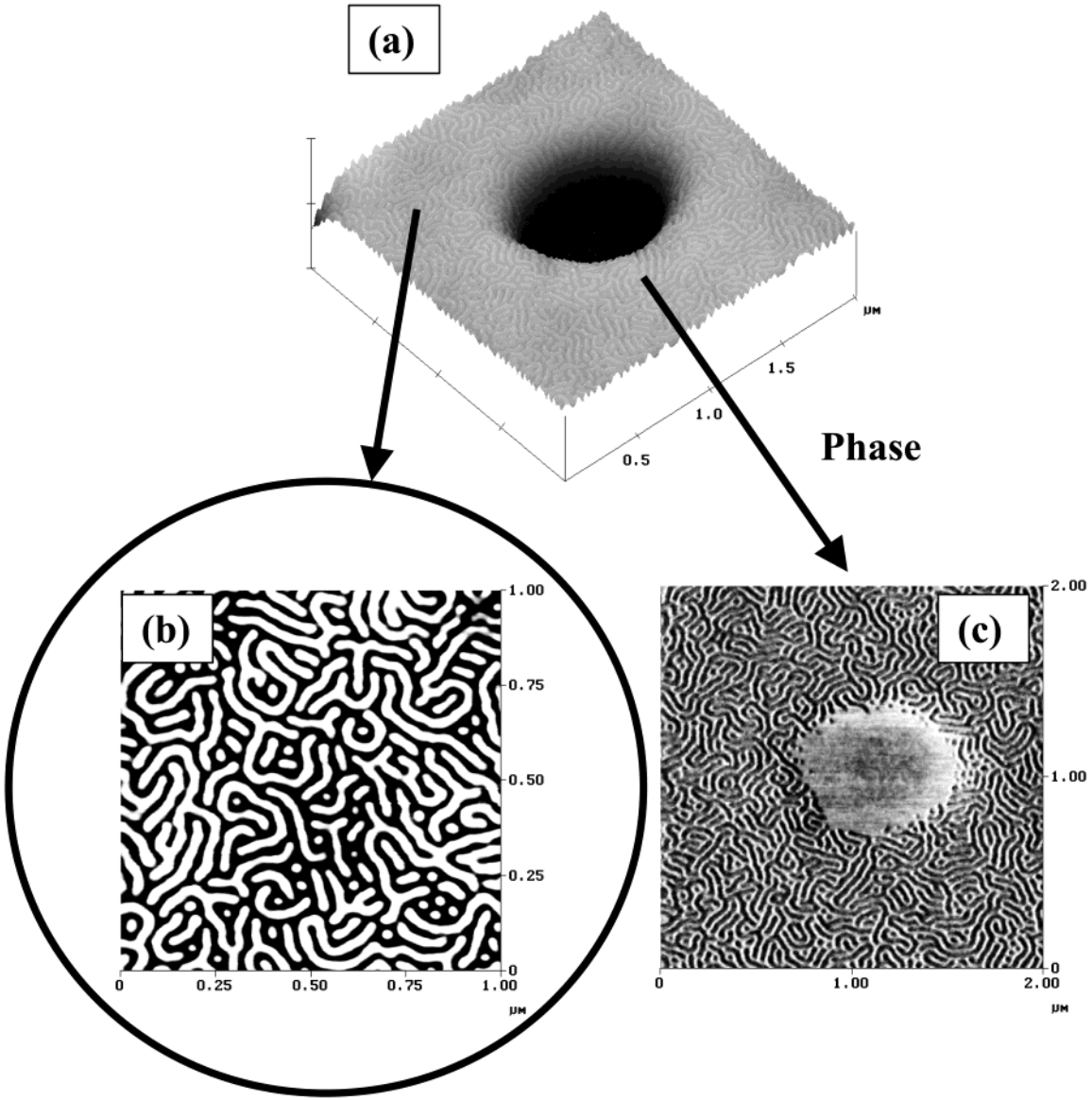

Figure 7. High-magnification SPM topographical (2 × 2 μm (a) and 1 × 1 μm (b)) and phase (2 × 2 μm (c)) images of SBS films spin-coated over PS-3(1). The formation of characteristic microphase-separated structures on the top of zeroth layer was observed. Vertical scale is 20 nm (a), 5.0 nm (b), and 70° (c). Bright parts correspond to higher features and phase shifts. Scanning at low set point.

The presence of islands and holes allows estimating the amount of the block copolymer involved in the formation of zeroth layer and, accordingly, the extent of penetration of PS block inside the polymer brush. Indeed, if the initial thickness of the block copolymer layer is known, the amount of the block copolymer "bounded" to the brush can be approximated by the following equation:

$$\Gamma_B = \Gamma_D - h_1 \rho f \qquad (9)$$

where Γ_B (mg/m^2) is the amount of the block copolymer involved in the zeroth layer, Γ_D = 29.5 mg/m^2 is the amount of SBS initially deposited on the surface calculated by eq 1, h_1 (nm) is height of islands or depth of holes, ρ is the SBS density (0.92 g/cm^3),[43] and f is the fraction of the surface covered with islands or occupied by the first layer (for the hole case). The product $h_1\rho f$ represents the amount of SBS material forming the islands or film with holes and not involved in the zeroth layer.

We analyzed SPM images (Figures 4 and 5) using NanoScope software to find the average height or depth (h_1) over a 50 μm × 50 μm area. Also, the fraction of the surface occupied by the first layer (f) was estimated. The data are presented in Table 3. We calculated the product $h_1\rho f$ to find the amount of SBS material that was not involved in the zeroth layer (Table 3). The calculated values were lesser then the amount of SBS initially deposited on the surface (Γ_D). This result also confirms the formation of the zeroth layer underneath the first layer. The height of islands and depth of the holes (h_1, Table 3) vary for different samples and are in the range from 17 to 34 nm. These values are less than the equilibrium spacing of the microdomain structure for the SBS copolymer, which was estimated to be around 45−50 nm.[13,21] We believe that this observation is associated with relatively low grafting density of the polymer brushes used in the present work and triblock nature of the SBS copolymer. In fact, one of the PS blocks of the copolymer constituting a zeroth layer may be incorporated within the polymer brush, while the

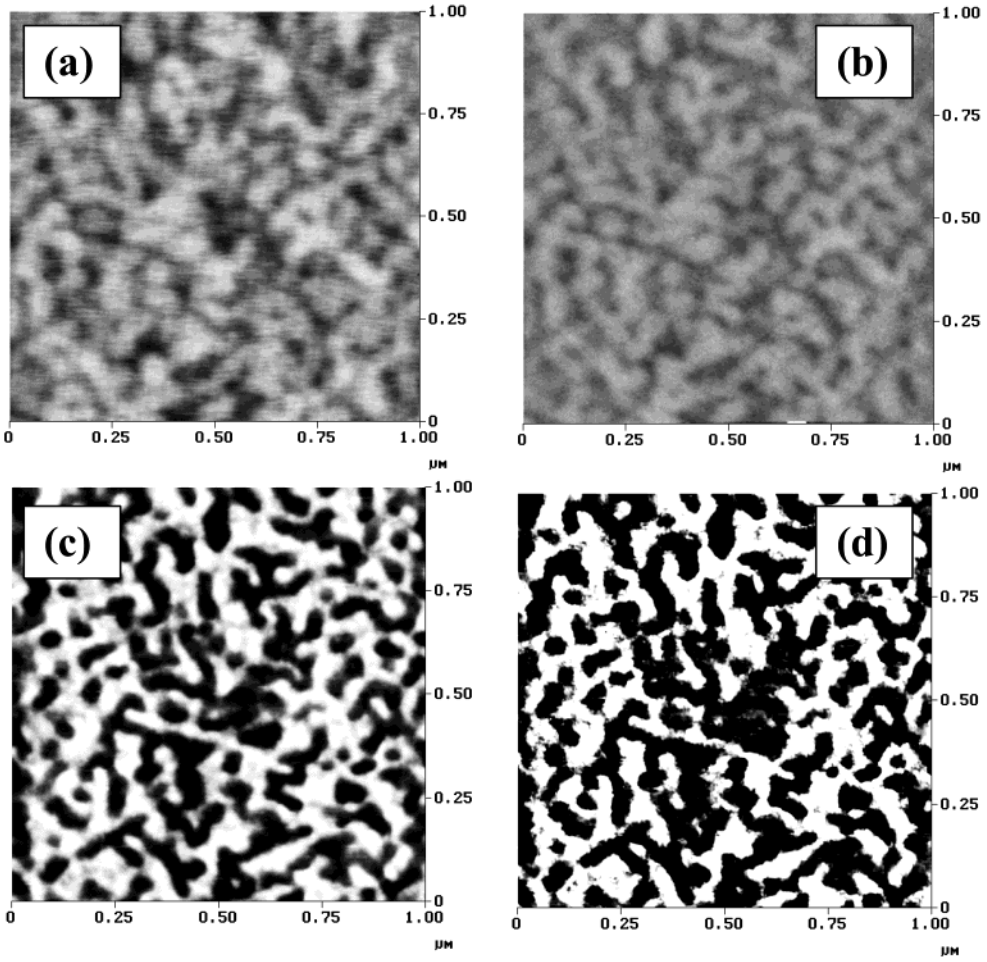

Figure 8. High-magnification SPM topographical (a, c) and phase images (b, d) of SBS films spin-coated over PS-3(2). Scanning at high (a, b) and low (c, d) set point. The images show surface (a, b) and internal (c, d) morphology of the zeroth layer. Vertical scale is 5.0 nm and 20° for topography and phase modes, respectively. Bright parts correspond to higher features and phase shifts.

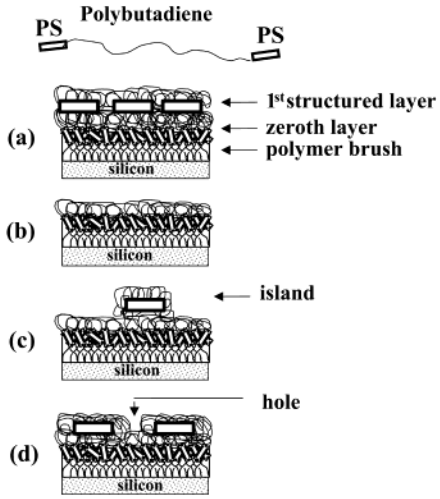

Figure 9. Schematic representation of morphology variation of SBS films deposited on PS grafted polymer layer.

other PS block of the same copolymer can be involved in the formation of the first layer. Indeed, we observed (Figure 8c,d) that the zeroth layer contains block copolymer chains with one PS block or both PS blocks penetrated inside the brush. The presence of different amounts of "free" PS blocks at the interface between the first and zeroth layers may lead to variation of the first layer thickness.

Table 3. Characteristics of SBS Films after Annealing

sample	h_1, nm	f	$h_1\rho f$	Γ_B (mg/m^2)	$N^{2/3}\sigma^{-2/3}$	$N(\sigma P)^{-1}$ or $N^{1/3}\sigma^{-1/3}$
PS-1(1)	33.5	0.33	10.2	19.3	223	17[a]
PS-1(2)	20.6	0.86	16.3	13.1	154	12.4[b]
PS-2(1)	28.0	0.58	14.9	14.5	584	70[a]
PS-3(1)	16.5	0.98	14.9	14.6	10651	5496[a]
PS-3(2)	0	0	0	29.5	5493	2035[a]
PS-4(1)	18.0	0.97	16.1	13.4	74238	101137[a]
PS-4(2)	24.0	0.48	10.6	18.9	33269	30341[a]

[a] $N(\sigma P)^{-1}$, since $P < N^{2/3}\sigma^{-2/3}$. [b] $N^{1/3}\sigma^{-1/3}$, since $P > N^{2/3}\sigma^{-2/3}$.

The amount of the block copolymer involved in the formation of the zeroth layer was estimated by eq 9. The results of the calculations are presented in Table 3. From 13 to 29.4 mg/m^2 of block copolymer constitutes the zeroth layer. Theory predicts that the length of penetration (λ) of homopolymer solvent inside the grafted polymer layer is proportional to N and σ:[16]

$$\lambda \propto N(\sigma P)^{-1}, \quad \text{for } P < N^{2/3}\sigma^{-2/3} \tag{10}$$

$$\lambda \propto N^{1/3}\sigma^{-1/3}, \quad \text{for } P > N^{2/3}\sigma^{-2/3} \tag{11}$$

The results of the calculations according to expressions 10 and 11 are presented in Table 3. The calculated penetration length significantly increases with the molar mass of the brush for our samples (Figure 10). From this viewpoint, the amount of SBS involved in the

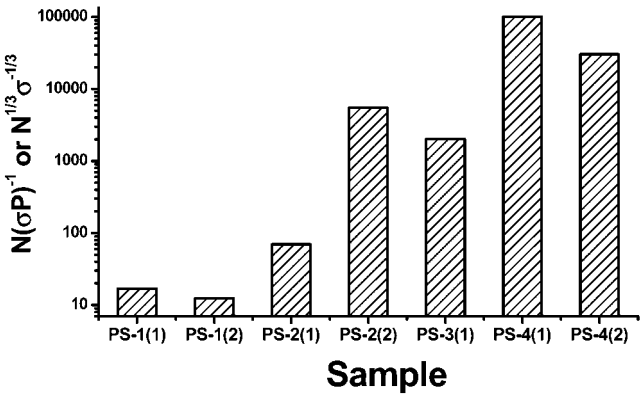

Figure 10. Variation of parameters $N(\sigma P)^{-1}$ and $N^{1/3}\sigma^{-1/3}$ for different samples. The parameters are proportional to the length of penetration (λ) of homopolymer solvent inside the grafted polymer layer.

formation of the zeroth layer should have higher values when the molar mass of the grafted polymer is increased. However, we do not observe this tendency experimentally for the samples studied here. We believe that this is caused by the different behaviors of homopolymer and block copolymer at the interface. For the homopolymer melt, the macromolecules can penetrate to a length higher than $2R_g$. However, the SBS macromolecules cannot penetrate as a whole inside the brush, since PS and PB are incompatible. Thus, only the PS block can be solubilized by the polymer brush. When the PS chains, constituting the brush, face PB block of the copolymer, the further incorporation of SBS into the brush should be arrested.

Numerous theoretical and experimental studies have described the solubilization of block copolymer segments by homopolymers, where the homopolymer is of similar chemistry as one of the block copolymer segments.[17,44] The driving force for the solubilization decreases with the degree of polymerization of the homopolymer. Thus, the amount of PS block incorporated ought to decrease with the increase of molar mass of the brush. Moreover, the solubilization occurs only when the molar mass of the homopolymer is equal to or lower than that of the compatible block copolymer segments. This condition should put a stop to the incorporation of SBS into the brush with the degree of polymerization higher than 201 (the degree of polymerization of PS block of SBS copolymer). Actually, for the high molar mass brushes, we should not observe any difference between the samples. But this trend was not also observed experimentally in our study. We believe that interplay between the two opposite trends predicted for grafted polymer/penetrating homopolymer and block copolymer/solubilizing homopolymer systems contributes to complicated process of the arrangement of the zeroth layer.

Grafting density is another parameter certainly involved in the formation of the zeroth layer. Within polymer layers made of the same polymer, Γ_B should be higher for the brush, which possesses lower density, since theoretically penetration depths vary in inverse proportion to σ (Table 2). Indeed, for low molar mass brush Γ_B decreases as the brush become denser. When the molar mass is higher (PS-3 and PS-4), we observed the opposite trend. The possible explanation of the observed phenomena is extremely low thickness (approximately 1 nm) of the low-density high molar mass grafted polymer layers. It may restrict the incorporation of the copolymer within the brush.

Conclusions

We found a strong effect of the underlying polystyrene brushes on the formation of the ultrathin SBS films on top of the brushes. The thickness of the films was kept constant, while the grafting density and molar mass of the polymer brush were varied over a wide range. We observed that a uniform zeroth layer (layer without internal ordered microphase separated structure) was formed on polymer brushes with widely variable grafting density and molar mass. It was found that both PS and PB blocks were present inside the zeroth layer. The first layer formed on top of the zeroth layer possessed the surface microstructure typical for the block copolymer in the bulk state. The polymer brushes were actively involved in the formation of the zeroth layer, and the microstructure of the block copolymer films was influenced by the grafting density and degree of the polymerization of the underlying grafted polymer layer. We observed significantly distinct morphologies for the copolymer films of the same thickness deposited on the different polymer brushes. Morphology of isolated islands, holes of different size, and intermediates between islands and holes as well as uniform zeroth layer developed during annealing. Our studies demonstrate that the morphology of ultrathin block copolymer film can be manipulated by the grafting density and molecular mass of the underlying brush.

Acknowledgment. This work is supported by Department of Commerce trough National Textile Center, M01-C03 Grant, and The National Science Foundation, CMS-0099868 Grant. The authors thank S. S. Minko for helpful and stimulating discussion, D. Julthongpiput for technical assistance in specimen prepration, and J. Pionteck for providing phthalic anhydride terminated PS.

References and Notes

(1) Huang, E.; Russell, T. P.; Harrison, C.; Chaikin, P. M.; Register, R. A.; Hawker, C. J.; Mays, J. *Macromolecules* **1998**, *31*, 7641.
(2) Mansky, P.; Russell, T. P.; Hawker, C. J.; Pitsikalis, M.; Mays, J. *Macromolecules* **1997**, *30*, 6810.
(3) Russell, T. P.; Menelle, A.; Anastasiadis, S. H.; Satija, S. K.; Majkrzak, C. F. *Macromolecules* **1991**, *24*, 6263.
(4) Kellogg, G. J.; Walton, D. G.; Mayes, A. M.; Lambooy, P.; Russell, T. P.; Galagher, P. D.; Satija, S. K. *Phys. Rev. Lett.* **1996**, *76*, 2503.
(5) Russell, T. P.; Mayes, A. M.; Bassereau, P. *Physica A* **1993**, *200*, 713.
(6) Konrad, M.; Knoll, A.; Krausch, G.; Magerle, R. *Macromolecules* **2000**, *33*, 5518.
(7) Mansky, P.; Liu, Y.; Huang, E.; Russell, T. P.; Hawker, C. *Science* **1997**, *275*, 1458.
(8) Huang, E.; Rockford, L.; Russell, T. P.; Hawker, C. J. *Nature (London)* **1998**, *395*, 757.
(9) Mansky, P.; Russel, T. P.; Hawker, C. J.; Mays, J.; Cook, D. C.; Satija, S. K. *Phys. Rev. Lett.* **1997**, *79*, 237.
(10) Huang, E.; Pruzinsky, S.; Russell, T. P.; Mays, J.; Hawker, C. J. *Macromolecules* **1999**, *32*, 5299.
(11) Huang, E.; Mansky, P.; Russell, T. P.; Harrison, C.; Chaikin, P. M.; Register, R. A.; Hawker, C. J.; Mays, J. *Macromolecules* **2000**, *33*, 80.
(12) Peters, R. D.; Yang, X. M.; Kim, T. K.; Nealey, P. F. *Langmuir* **2000**, *16*, 9620.
(13) Harrison, C.; Chaikin, P. M.; Huse, D. A.; Register, R. A.; Adamson, D. H.; Daniel, A.; Huang, E.; Mansky, P.; Russell, T. P.; Hawker, C. J.; Egolf, D. A.; Melnikov, I. V.; Bodenschatz, E. *Macromolecules* **2000,** *33*, 857.
(14) Harrison, C.; Park, M.; Chaikin, P. M.; Register, R. A.; Adamson, D. H.; Yao, N. *Polymer* **1998**, *39*, 2733.
(15) Reiter, G.; Auroy, P.; Auvray, L. *Macromolecules* **1996**, *29*, 2150.

(16) Gay, C. *Macromolecules* **1997**, *30*, 5939.
(17) Liu, Y.; Rafailovich, M. H.; Sokolov, J.; Schwarz, S. A.; Zhong, X.; Eisenberg, A.; Kramer, E. J.; Sauer, B. B.; Satija, S. *Phys. Rev. Lett.* **1994**, *73*, 440.
(18) Luzinov, I.; Julthongpiput, D.; Malz, H.; Pionteck, J.; Tsukruk, V. V *Macromolecules* **2000**, *33*, 1043.
(19) Zhang, Q.; Tsui, O. K. C.; Du, B.; Zhang, F.; Tang, T.; He, T. *Macromolecules* **2000**, *33*, 9561.
(20) Tsukruk, V. V.; Luzinov, I.; Julthongpiput, D. *Langmuir* **1999**, *15*, 3029. Luzinov, I.; Julthongpiput, D.; Liebmann-Vinson, A.; Cregger, T.; Foster, M. D.; Tsukruk, V. V. *Langmuir* **2000**, *16*, 504.
(21) Helfand, E.; Wasserman, Z. R. *Macromolecules* **1976**, *9*, 879. Helfand, E.; Wasserman, Z. R. *Macromolecules* **1978**, *11*, 960.
(22) Tsukruk, V. V. *Rubber Chem. Technol.* **1997**, *70* (3), 430. Tsukruk, V. V.; Reneker, D. H. *Polymer* **1995**, *36*, 1791.
(23) Ratner, B., Tsukruk, V. V., Eds.; *Scanning Probe Microscopy of Polymers; ACS Symp. Ser.* **1998**, *694*.
(24) Magonov, S. N.; Cleveland, J.; Elings, V.; Denley, D.; Whangbo, M.-H. *Surf. Sci.* **1997**, *389*, 201.
(25) Bar, G.; Thomann, Y.; Brandsch, R.; Cantow, H.-J.; Whangbo, M.-H. *Langmuir* **1997**, *13*, 3807.
(26) Pickering, J. P.; Vancso, G. J. *Polym. Bull. (Berlin)* **1998**, *40*, 549.
(27) *27.Scanning Probe Microscopy: Training Notebook*; Digital Instruments, Veeco Metrology Group, 2000; p 40.
(28) Henn, G.; Bucknall, D. G.; Stamm, M.; Vanhoorne, P.; Jerome, R. *Macromolecules* **1996**, *29*, 4305.
(29) Van Krevelen, D. W. *Properties of Polymers*; Elsevier: Amsterdam, 1997.
(30) Siqueira, D. F.; Kohler, K.; Stamm, M. *Langmuir* **1995**, *11*, 3092.
(31) Sperling, L. H. *Introduction to Physical Polymer Science*; John Wiley & Sons: New York, 1992.
(32) Zhulina, E. B.; Birshtein, T. M.; Priamitsyn, V. A.; Klushin, L. I. *Macromolecules* **1995**, *28*, 8612.
(33) Koutos, V.; van der Vegte, E. W.; Hadziioannou, G. *Macromolecules* **1999**, *32*, 1233.
(34) Koutos, V.; van der Vegte, E. W.; Pelletier, E.; Stamouli, A.; Hadziioannou, G. *Macromolecules* **1997**, *30*, 4719. Koutos, V.; van der Vegte, E. W.; Grim, P. C. M.; Hadziioannou, G. *Macromolecules* **1998**, *31*, 116.
(35) Singh, C.; Zhulina, E. B.; Gersappe, D.; Pickett, G. T.; Balazs, A. C. *Macromolecules* **1996**, *29*, 7637.
(36) Luzinov, I.; Minko, S.; Senkovsky, V.; Voronov, A.; Hild, S.; Marti, O.; Wilke, W. *Macromolecules* **1998**, *31*, 3945.
(37) Bar, G.; Thomann, Y.; Whangbo, M.-H. *Langmuir* **1998**, *14*, 1219.
(38) Magonov, S. N.; Elings, V.; Whangbo, M.-H. *Surf. Sci.* **1997**, *375*, 385.
(39) Hasegawa, H.; Hashimoto, H. *Polymer* **1992**, *33*, 475. Chen, J. T.; Thomas, E. L. *J. Mater. Sci.* **1996**, *31*, 2531.
(40) de Gennes, P. G. *Macromolecules* **1980**, *13*, 1069.
(41) Aubouy, M.; Fredrikson, G. H.; Pincus, P.; Raphaël, E. *Macromolecules* **1995**, *28*, 2979.
(42) Yokoyama, H.; Mates, T. E.; Kramer, E. J. *Macromolecules* **2000**, *33*, 1888.
(43) Kraton polymers and compound. Typical properties guide. Shell Chemical Company, 1996.
(44) Winey, K. I.; Thomas, E. L.; Fetters, L. J. *Macromolecules* **1991**, *24*, 6182. Kinning, D. J.; Winey, K. I.; Thomas, E. L. *Macromolecules* **1988**, *21*, 3502. Tanaka, H.; Hasegava, H.; Hashimoto, T. *Macromolecules* **1991**, *24*, 240. Jeon, K. J.; Roe, R. J. *Macromolecules* **1994**, *27*, 2439. Adedeji, A.; Hudson, S. D.; Jamieson, A. M. *Polymer* **1997**, *38*, 737.

MA0205818